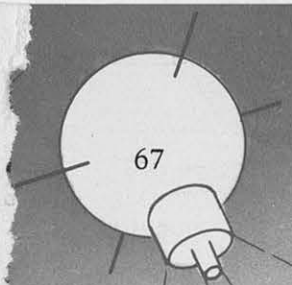

SATELLITE & MESOMETEOROLOGY RESEARCH PROJECT

Department of the Geophysical Sciences
The University of Chicago

MESOSCALE ASPECTS OF OROGRAPHIC INFLUENCES ON FLOW AND PRECIPITATION PATTERNS

by

Tetsuya Fujita

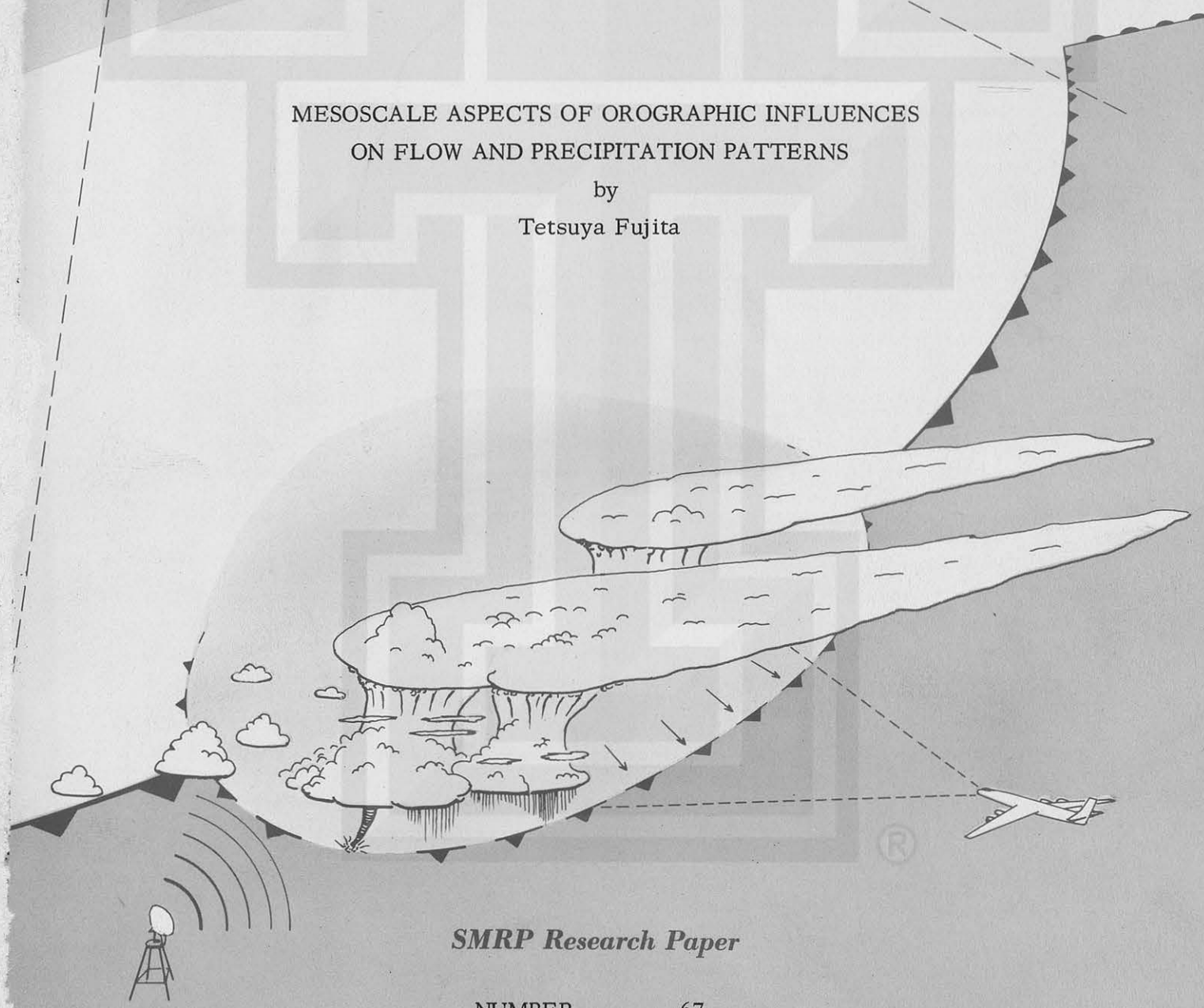

SMRP Research Paper

NUMBER 67

June 1967

MESOMETEOROLOGY PROJECT --- RESEARCH PAPERS

1.* Report on the Chicago Tornado of March 4, 1961 - Rodger A. Brown and Tetsuya Fujita

2.* Index to the NSSP Surface Network - Tetsuya Fujita

3.* Outline of a Technique for Precise Rectification of Satellite Cloud Photographs - Tetsuya Fujita

4.* Horizontal Structure of Mountain Winds - Henry A. Brown

5.* An Investigation of Developmental Processes of the Wake Depression Through Excess Pressure Analysis of Nocturnal Showers - Joseph L. Goldman

6.* Precipitation in the 1960 Flagstaff Mesometeorological Network - Kenneth A. Styber

7.** On a Method of Single- and Dual-Image Photogrammetry of Panoramic Aerial Photographs - Tetsuya Fujita

8. A Review of Researches on Analytical Mesometeorology - Tetsuya Fujita

9. Meteorological Interpretations of Convective Nephsystems Appearing in TIROS Cloud Photographs - Tetsuya Fujita, Toshimitsu Ushijima, William A. Hass, and George T. Dellert, Jr.

10. Study of the Development of Prefrontal Squall-Systems Using NSSP Network Data - Joseph L. Goldman

11. Analysis of Selected Aircraft Data from NSSP Operation, 1962 - Tetsuya Fujita

12. Study of a Long Condensation Trail Photographed by TIROS I - Toshimitsu Ushijima

13. A Technique for Precise Analysis of Satellite Data; Volume I - Photogrammetry (Published as MSL Report No. 14) - Tetsuya Fujita

14. Investigation of a Summer Jet Stream Using TIROS and Aerological Data - Kozo Ninomiya

15. Outline of a Theory and Examples for Precise Analysis of Satellite Radiation Data - Tetsuya Fujita

16. Preliminary Result of Analysis of the Cumulonimbus Cloud of April 21, 1961 - Tetsuya Fujita and James Arnold

17. A Technique for Precise Analysis of Satellite Photographs - Tetsuya Fujita

18. Evaluation of Limb Darkening from TIROS III Radiation Data - S.H.H. Larsen, Tetsuya Fujita, and W.L. Fletcher

19. Synoptic Interpretation of TIROS III Measurements of Infrared Radiation - Finn Pedersen and Tetsuya Fujita

20. TIROS III Measurements of Terrestrial Radiation and Reflected and Scattered Solar Radiation - S.H.H. Larsen, Tetsuya Fujita, and W.L. Fletcher

21. On the Low-level Structure of a Squall Line - Henry A. Brown

22. Thunderstorms and the Low-level Jet - William D. Bonner

23. The Mesoanalysis of an Organized Convective System - Henry A. Brown

24. Preliminary Radar and Photogrammetric Study of the Illinois Tornadoes of April 17 and 22, 1963 - Joseph L. Goldman and Tetsuya Fujita

25. Use of TIROS Pictures for Studies of the Internal Structure of Tropical Storms - Tetsuya Fujita with Rectified Pictures from TIROS I Orbit 125, R/O 128 - Toshimitsu Ushijima

26. An Experiment in the Determination of Geostrophic and Isallobaric Winds from NSSP Pressure Data - William Bonner

27. Proposed Mechanism of Hook Echo Formation - Tetsuya Fujita with a Preliminary Mesosynoptic Analysis of Tornado Cyclone Case of May 26, 1963 - Tetsuya Fujita and Robbi Stuhmer

28. The Decaying Stage of Hurricane Anna of July 1961 as Portrayed by TIROS Cloud Photographs and Infrared Radiation from the Top of the Storm - Tetsuya Fujita and James Arnold

29. A Technique for Precise Analysis of Satellite Data, Volume II - Radiation Analysis, Section 6. Fixed-Position Scanning - Tetsuya Fujita

30. Evaluation of Errors in the Graphical Rectification of Satellite Photographs - Tetsuya Fujita

31. Tables of Scan Nadir and Horizontal Angles - William D. Bonner

32. A Simplified Grid Technique for Determining Scan Lines Generated by the TIROS Scanning Radiometer - James E. Arnold

33. A Study of Cumulus Clouds over the Flagstaff Research Network with the Use of U-2 Photographs - Dorothy L. Bradbury and Tetsuya Fujita

34. The Scanning Printer and Its Application to Detailed Analysis of Satellite Radiation Data - Tetsuya Fujita

35. Synoptic Study of Cold Air Outbreak over the Mediterranean using Satellite Photographs and Radiation Data - Aasmund Rabbe and Tetsuya Fujita

36. Accurate Calibration of Doppler Winds for their use in the Computation of Mesoscale Wind Fields - Tetsuya Fujita

37. Proposed Operation of Intrumented Aircraft for Research on Moisture Fronts and Wake Depressions - Tetsuya Fujita and Dorothy L. Bradbury

38. Statistical and Kinematical Properties of the Low-level Jet Stream - William D. Bonner

39. The Illinois Tornadoes of 17 and 22 April 1963 - Joseph L. Goldman

40. Resolution of the Nimbus High Resolution Infrared Radiometer - Tetsuya Fujita and William R. Bandeen

41. On the Determination of the Exchange Coefficients in Convective Clouds - Rodger A. Brown

* Out of Print
** To be published

(Continued on back cover)

SATELLITE AND MESOMETEOROLOGY RESEARCH PROJECT
Department of the Geophysical Sciences
The University of Chicago

MESOSCALE ASPECTS OF OROGRAPHIC INFLUENCES ON FLOW AND PRECIPITATION PATTERNS

by
Tetsuya Fujita

SMRP Research Paper No. 67
June 1967

The research reported in this paper has been sponsored by the Meteorological Satellite Laboratory, ESSA, under Grant Cwb WBG-34 Research. The collection of precipitation data from the Flagstaff mesometeorological network in 1960 and 1961 was supported by the U.S. Air Force Office of Aerospace Research (GRD) under Contract AF 19(604)-7259.

MESOSCALE ASPECTS OF OROGRAPHIC INFLUENCES ON FLOW AND PRECIPITATION PATTERNS[1]

Tetsuya Fujita

Department of the Geophysical Sciences
The University of Chicago
Chicago, Illinois

ABSTRACT

Since horizontal dimensions of orography in relation to cloud formation and development are mostly in the mesoscale, we usually observe mesoscale nephsystems in areas with topographic influences. In addition to their barrier effects, mountains during the daytime act as effective high-level heat sources or as cloud generators. At night, however, they suppress the cloud formation and act as cloud dissipators. When these effects are combined with the height of the convective cloud base, which could be either higher or lower than that of the mountains, the patterns of orographic nephsystems and precipitation are quite complicated. By using actual cases of cloud and precipitation measurements, detailed climatological and mesosynoptic patterns of clouds and precipitation are discussed.

1. Orographic Clouds and Precipitation in Relation to the Base of Convective Clouds

It is well-known that the worldwide rainfall patterns are closely related to the large-scale flow patterns and the orography which blocks the flow in various ways. Even though the role of the mountains upon natural stimulation of precipitation is not fully understood, the difference between the height of the convective cloud base and that of mountain tops results in significant variation in the rainfall patterns on and around the mountains.

When the condensation level or cloud base is considerably lower than the mountain tops, cloud growth and precipitation take place on the upwind side of the

---

[1] The research reported in this paper has been sponsored by the Meteorological Satellite Laboratory, ESSA, under Grant Cwb WBG-34 Research. The collection of precipitation data from the Flagstaff mesometeorological network in 1960 and 1961 was supported by the U.S. Air Force Office of Aerospace Research (GRD) under Contract AF 19(604)-7259.

mountains. The effect of solar radiation becomes insignificant as soon as the upwind slopes are covered with thick convective clouds with high albedo.

The mechanical lifting of moist air is the most important mechanism for the release of latent heat of condensation when the stratification is conditionally unstable. Elliott and Schaffer (1962) showed that the ratio of amounts of mountain and flat-ground precipitation decreases appreciably with increasing air-mass stability, suggesting that the orographic stimulation of precipitation does not occur when the air mass is stable.

Even small mountains blocking a rapid flow of moisture in the tropics, such as that accompanying hurricanes and typhoons, result in a significant amount of precipitation on the upwind side of the mountains. Figure 1 shows an example of orographic rainfall over Japan under the influence of Typhoon Bess in August, 1963. Winds plotted in the standard form in the lower figure represent velocities of the radar echoes computed by Fujita et. al. (1967). The height of the cumulus base on the upwind side varies between 1000 and 2000 ft while the mountains are as high as 5000 ft. It is of interest to see in the upper chart that along the Pacific coast the one-hour rainfall ending at 0500Z is only several millimeters. Heavy rainfall, up to 18 mm, is seen only on the upwind slope of the mountains. No more than a trace of rainfall is reported from the downwind regions, thus showing the effective blocking of precipitation by such relatively low mountains.

When the condensation level is located near or above the mountain tops, convective clouds forming on the peak or over the leeward side of the mountain produce precipitation as they drift away from the ridge line. As seen in Fig. 2, such cloud formations are quite common over dry regions. Note that clouds over Baja California extend northeast from the ridge line of the Sierra de Juárez and that similar cloud formations in Nevada, Utah, and Arizona have the same relative location with respect to orography.

In such cases, the heating of the mountain slopes plays an important role upon the acquisition of buoyancy by orographic cumuli. Especially when the low-level wind is southerly, the orographic clouds forming and developing above the northern slopes of mountains do not effectively shield the solar radiation reaching the southern slopes along which the heated air travels upward.

Braham and Draginis (1960), and Silverman (1960), using data obtained from an instrumented Air Force aircraft, made detailed analyses of the moisture and temperature patterns above the Santa Catalina Mountains north of Tucson, Arizona.

They revealed that the heated moist air, because of the lifting effect of the barrier and the high-level heating effect of the mountain, reached 3000 to 5000 ft above the mountain-top level after the slope was heated by the morning sun.

The growth of cumuli clouds after their formation above mountain-top level was investigated by Glass and Carlson (1963), who made detailed photogrammetric analyses of cumulus development over the San Francisco Mountains north of Flagstaff, Arizona. Their results indicate that initial clouds with their bases at 17,500 - 20,000 ft formed a few tenths of a mile downwind from the 12,680 ft peak. After the formation, each cloud drifted away from the source region while increasing its volume as much as 10 times. They studied mostly small cumuli which were eroded away after about 10 minutes. These clouds consisted mostly of up-slope thermals which were mixed with environmental air several thousand feet above the mountain tops. It is very unlikely that these small clouds would receive a continuous supply of moist air from the lower levels on the downwind side of the mountain. If one of these cumuli developed into a huge cumulonimbus, it would maintain its circulation practically independent of the orography which gave rise to the development of the initial cloud. Thus, a large storm could move away from the mountains for a great distance downwind.

2. Distribution of Rainfall Patterns around Isolated Mountains

In an attempt to investigate pressure disturbances associated with the orographic precipitation around the San Francisco Mountains of Arizona, a mesometeorological network of stations was established and operated by the University of Chicago and sponsored by the U.S. Air Force. Figure 3 shows the area dominated by the San Francisco Mountains in northern Arizona.

Long before the attempt by the Air Force to study orographic convection in the Flagstaff area, Indians knew and told the participating scientists that their rainy season would start as soon as the traditional annual Rain Dance was performed at Flagstaff early in July. Both 1960 and 1961 networks began to operate shortly after the day of the Rain Dance, which actually signalled the beginning of the moist spell.

The total precipitation amounts for July 16-29, 1960, plotted and contoured in Fig. 4 clearly show a maximum directly over the mountains, and are surrounded by a ring-shaped zone of relatively low total amounts (see black dots circling the mountains). Outside this ring were scattered areas of high values up to 2.2 inches.

In order to learn whether the 1960 pattern of orographic rainfall represents a general distribution or not, a second and more extensive network was established in 1961. The number of raingauges was increased from 150 to 220. The pattern of the total precipitation turned out to be very similar to that obtained in 1960. The total amount of rainfall in the 1961 period was about twice that of the previous year, due partially to more days of operation, which were increased from 14 to 19 days, and to the increased convective activity. Nevertheless, the low total-precipitation ring surrounding the mountains appeared practically the same as in 1960.

To represent variation in the rainfall as a function of the distance from the mountain, six pie-shaped areas were constructed by drawing six azimuths, 000°, 060°, 120°, 180°, 240°, and 300°, radiating from the center of the mountain. The scatter diagram (Fig. 6) obtained by plotting the precipitation within each pie-shaped area reveals the existence of a low total-precipitation area at a distance of about 8 nm from the mountain. A ring of maximum rainfall is also seen along the radius of 10 to 12 nm. This evidence poses the question as to the cause of these rings of minimum and maximum precipitation.

Fujita, Styber, and Brown's (1962) study of daily precipitation during the 1960 season indicated that the over-mountain rainfall mostly occurred on the days with low wind speeds and that the distant rainfall, 10 to 12 nm from the mountain center, fell quite often at night. Braham (1958) concluded in his study of cumulus clouds in Arizona that every one of the cloud parameters showed marked day-by-day variations. His statement is very important since it implies difficulties in explaining the daily regime of orographic convection from the broad synoptic conditions.

From this we may assume that over-mountain precipitation is predominant when straight convection takes place under the influence of relatively low wind speeds. A distant rainfall may occur at night when the mountains are cold, thus acting as cloud dissipators rather than cloud generators. If a very high cloud base and relatively high winds occur simultaneously, it is likely that convective clouds will drift away some distance from the mountains, producing precipitation far away from the mountains. Thus, somehow, a minimum amount of precipitation is received along a ring of about 15 mi in diameter circling the mountains.

3. Influence of Airflow and Moisture

It is the common belief in northern Arizona that rainfall occurs when moist air, mostly from the southeast, blows against the plateaus and mountains. To

obtain a quantitative relationship between the precipitation, the airflow, and the humidity, the winds aloft and relative humidities measured at Flagstaff are presented in Figs. 7 and 8, respectively. At the upper part of each figure is the variation of mean daily precipitation obtained by adding total daily amounts from all network stations and then dividing the total by the number of stations. The mean daily precipitation, therefore, gives approximately the mean precipitation which fell each day over the network area.

An overall inspection of these figures does not lead to a conclusion as to a cause and effect relationship. Therefore, the daily means of wind speed and relative humidity between the surface and the 10,000 ft level were computed from upper-air data taken early each morning before the onset of daily orographic convection. These values are entered in Figs. 7 and 8 below the line representing the station elevation.

The standard presentation of 3-parameter correlation shown in Fig. 9 requires more observed values in order to find a conclusive relationship. Nonetheless, the scatter diagram of rainfall amounts vs. relative humidity permits us to draw a crude but reasonable straight line, indicating that there would be little rain when the mean relative humidity is less than 10 to 15%. In case the humidity exceeds 80% it is likely there will be more than 0.2 inches of rain no matter how weak the wind speed. Due to the fact that there were no cases of high wind speed when the humidity was 60% or more, it is not feasible to extrapolate the precipitation which would occur under high-wind and high-humidity conditions. For low-humidity cases, however, the precipitation tends to increase with increasing wind speed.

The most reasonable empirical formula for estimating mean precipitation, R, from V, the wind speed, and H, the relative humidity would be

$$R = \frac{1}{3}(H-0.1)(1+0.01V)$$

$$\text{and} \quad R = 0 \qquad \text{when} \quad H < 0.1$$

where R is expressed in inches and V in knots. The line of a specific value of in this formula is a rectangular hyperbola with V and H axes translated to V = −100 kt and H = 0.1, respectively.

4. Split of a Thunderstorm in the Wake Flow of the San Francisco Mountains

Due to the barrier and heating effects of the isolated peaks one would expect

some unusual characteristics of thunderstorms in the wake region of the mountains. To monitor such thunderstorms, a time-lapse 16-mm camera was placed on the rim of Meteor Crater pointing toward the San Francisco Mountains, about 40 mi away. Inspection of a large number of the movies thus obtained during 1961 operations revealed the fact that a precipitation area observed beneath a cumulonimbus cloud travelling downwind generally split into two separate precipitation areas.

A series of pictures enlarged from the film taken on July 19, 1961, is shown in Fig. 10. Although the exposures were made for every 15 sec, frames presented in the figure were selected at about 15-min intervlas. The first cumulus over the mountain appeared at 0845 MST. After repeating the processes as described by Glass and Carson (1963), a towering cumulus stage was reached around 1000 MST. A few minutes later, both anvil and virga extended from the cloud.

Shortly after 1030 MST the rain area in the movie widened rapidly until it split into two parts. Then the one on the left moved almost toward the camera. A close inspection showed that the left part moved back slightly toward the direction of the peaks when viewed from the movie camera. The right part, on the other hand, moved to the right, very quickly moving out of sight shortly after 1130 MST.

A MRI SX6 radar with 3.2 cm wave length constructed and operated by Meteorological Research Incorporated, Altadena, California, was not turned on until 1127 MST, because the thunderstorm in question was previously hidden behind Elden Mountain when viewed from Flagstaff Airport, the site of the radar.

When the radar picture taken at 1130 MST and an enlarged cloud picture from Meteor Crater are combined precisely as shown in Fig. 11, it is found that the shape of the echoes from the split rain showers displayed rotational characteristics. This was especially true for the one on the right, viewed from the movie camera, which showed an anticyclonic rotation lasting for over 30 min after the radar was turned on. The other showed a slight cyclonic curvature. The estimated paths of the echo before and after the split revealed a remarkable resemblance with the echo-split phenomenon studies by Fujita and Grandoso (1966). They obtained a numerical model which included a pair of thunderstorms which rotated in opposite directions. If their concept of split-echo phenomenon is applied to this observational evidence, it may be concluded that an area of wake flow behind the San Francisco Mountains extends more than 30 mi downwind.

A schematic-plan view of an estimated wake flow is shown in Fig. 12. Note that a zone of anticyclonic vorticity along the northern boundary of the wake and

its counterpart zone of cyclonic vorticity along the southern boundary are produced as a result of the barrier effect. When a developing thunderstorm moves over this area sucking up the air from the wake region, the left-hand portion (facing the direction of motion) and the right-hand part will quickly accumulate negative and positive vorticities, respectively. Thus, the storm rapidly splits into one with cyclonic, and the other with anticyclonic rotation.

A Flagstaff sounding taken at 1235 MST, July 19, 1961, is shown in Fig. 12. It is seen that the layers up to 21,000 ft, slightly above the cloud base, were practically adiabatic with the moisture decreasing slightly with increasing height. This layer is topped by a thick layer of dry air moving from west to northwest at 12 to 15 kt. The temperature curve for the morning sounding, released at 0840, showed little difference from that of the noon sounding. Therefore, the flow probably remained unchanged during the morning hours, acting in favor of the establishment of a steady-state flow.

5. Summary and Conclusions

The importance of the height of the convective cloud base in relation to that of the orography blocking the flow has been discussed, based on several examples. In interpreting satellite photographs it is always necessary to keep such regimes of convection in mind because the locations of clouds relative to the mountains vary according to the height of the cloud base.

The orographic precipitation around the San Francisco Mountains was studied in detail, and a related ring of light precipitation surrounding the mountains was found to exist during both the 1960 and 1961 operations. In order to explain such a distribution, the group of mountains is assumed to act as a cloud generator in daytime and as a cloud dissipator at night. Finally, the wake effect of the mountains, which gives rise to the echo split phenomenon as proposed by Fujita and Grandoso (1966), was discussed. A large number of satellite pictures over Arizona taken in July and August were examined in an attempt to find patterns of clouds associated with the wake flow behind mountains. However, no conclusive evidence of wake flow was found. The regions of wake flow in satellite pictures as described by Hubert and Lehr (1967) are considerably more extensive than the island which blocks the flow. These islands usually extend above the top of a shallow stable layer, but the mountains in Arizona block only the lower portion of an adiabatic layer over 10,000 ft thick.

When the nature of such wake flows is clarified in general, it will become feasible to use satellite pictures for the establishment of both barrier and heating effects of topography upon the mesoscale orographic convection.

REFERENCES

Braham, R. R., 1958: Cumulus cloud precipitation as revealed by radar---Arizona 1955. J. Meteor., 15, 75-83.

_____, and M. Draginis, 1960: Roots of orographic cumuli. J. Meteor., 17, 214-226.

Elliott, R. D., and R. W. Shaffer, 1962: The development of quantitative relationships between orographic precipitation and air-mass parameters for use in forecasting and cloud seeding evaluation. J. Appl. Meteor., 1, 218-228.

Fujita, T., K. A. Styber, and R. A. Brown, 1962: On the mesometeorological field studies near Flagstaff, Arizona. J. Appl. Meteor., 1, 26-42.

_____, and H. Grandoso, 1966: Split of a thunderstorm into anticyclonic and cyclonic storms as determined from numerical model experiments. SMRP Res. Paper No. 62, 43 pp. (Available from SMRP).

_____, T. Izawa, K. Watanabe, and I. Imai, 1967: A model of typhoons accompanied by inner and outer rainbands. J. Appl. Meteor., 6, 3-19.

Glass, M., and T. N. Carlson, 1963: The growth characteristics of small cumulus clouds. J. Atmos. Sci., 20, 397-406.

Hubert, L. F., and P. E. Lehr, 1967: Weather Satellites. Blaisdell Publishing Company, Waltham, Mass., 120 pp.

Silverman, B. A., 1960: The effect of a mountain on convection. Cumulus Dynamics. Pergamon Press, New York, 4-27.

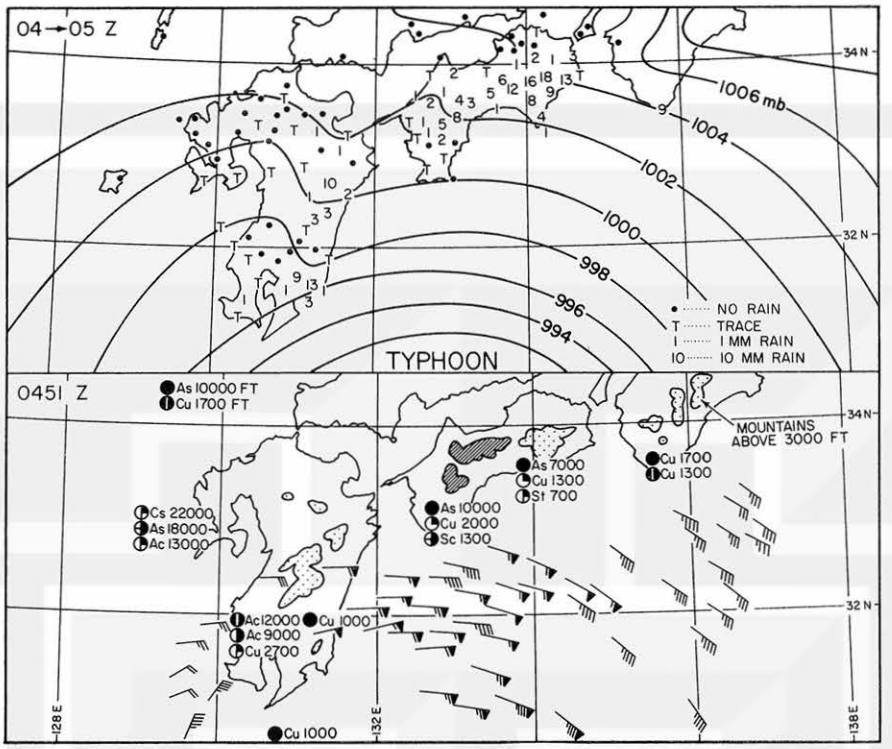

Fig. 1. An example of orographic precipitation with the convective cloud base much lower than that of the mountain barrier. Upper: Hourly precipitation in mm between 0400 and 0500 GMT 8 August 1963. Lower: Cloud bases observed at 0500 GMT from ground stations in southern Japan and the velocities of radar echoes at 0451 GMT from Fujita et. al. (1967).

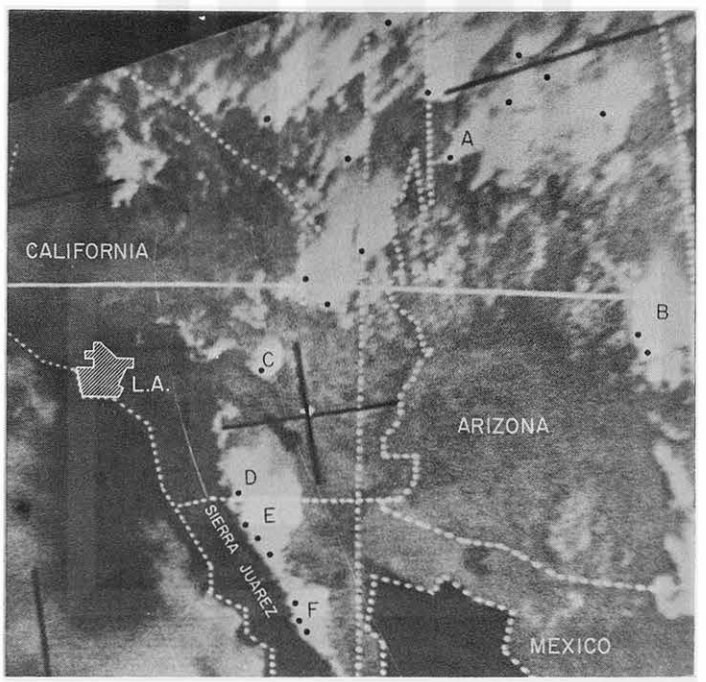

Fig. 2. An example of orographic clouds with their bases at or above the mountain-top level. Large cumulonimbi are identified by letters A through F. Black dots designate the positions of the mountain peaks, which are assumed to be the source regions. ESSA I picture taken at 1407 MST 23 July 1966.

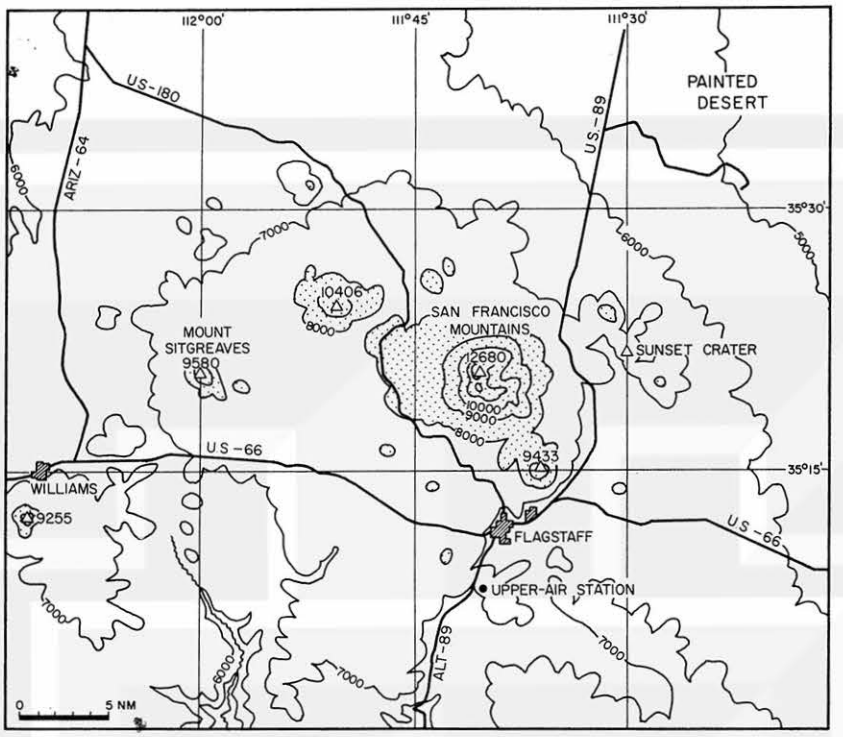

Fig. 3. Topography around the San Francisco Mountains in northern Arizona, where a raingauge network was operated during 1960 and 1961 seasons.

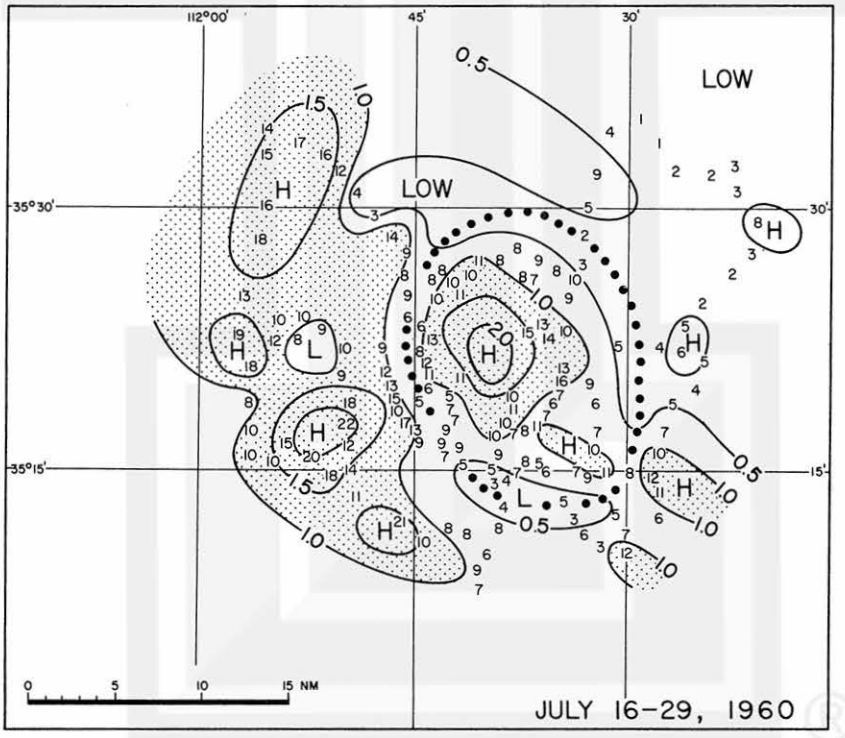

Fig. 4. Total precipitation during the period July 16-29, 1960, measured at about 150 stations around the San Francisco Mountains. Amounts were plotted in 0.1-inch units and contoured for every 0.5 inch. H and L designate high and low values, respectively. Black dots circling a high rainfall area over the mountains indicate a ring of low precipitation.

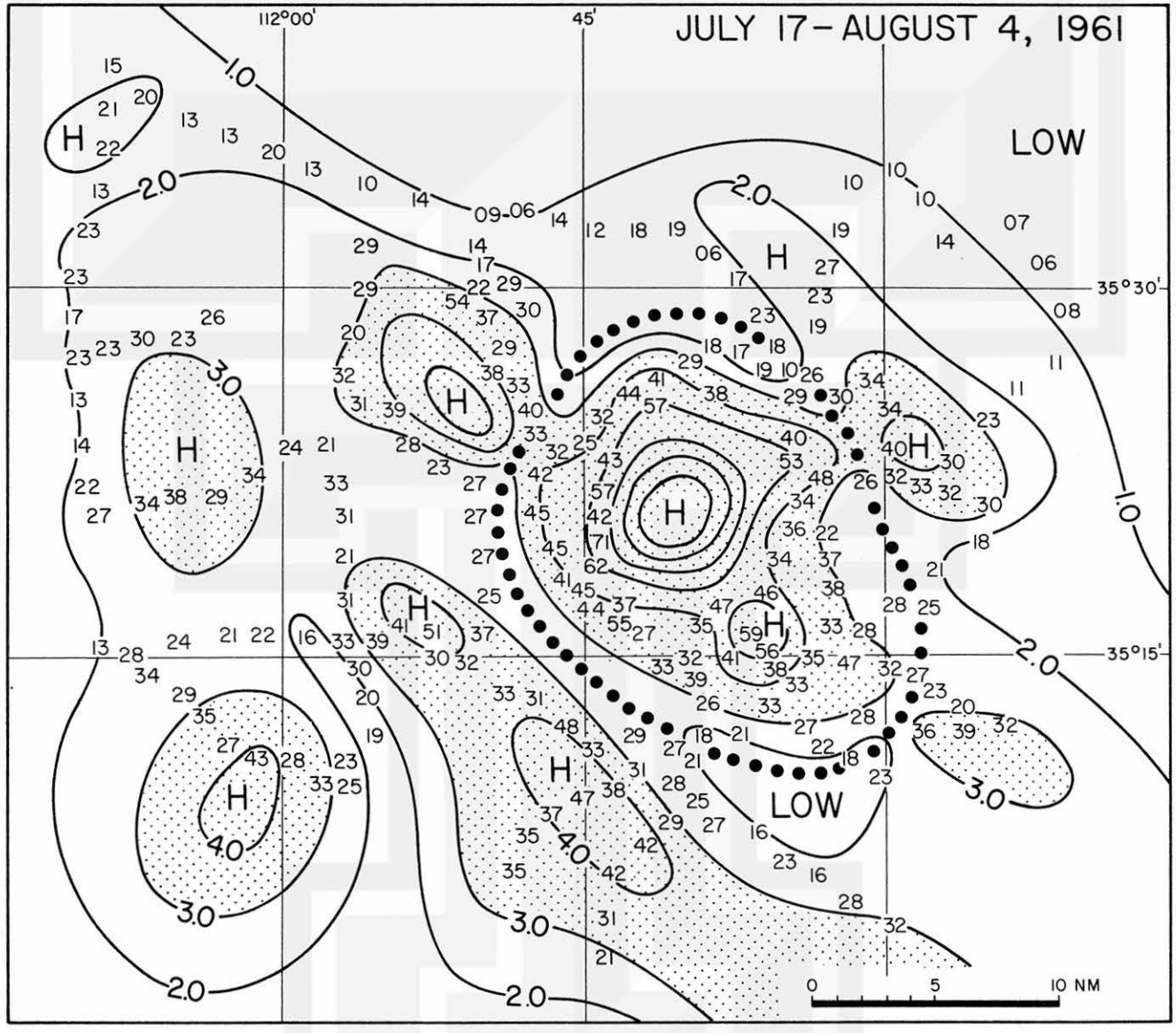

Fig. 5. Total precipitation during July 17-August 4, 1961, measured at about 220 stations. Amounts are shown in increments of 0.1 inch, and isohyets were drawn at one-inch intervals. Note that a ring of low precipitation around the mountain existed again in 1961.

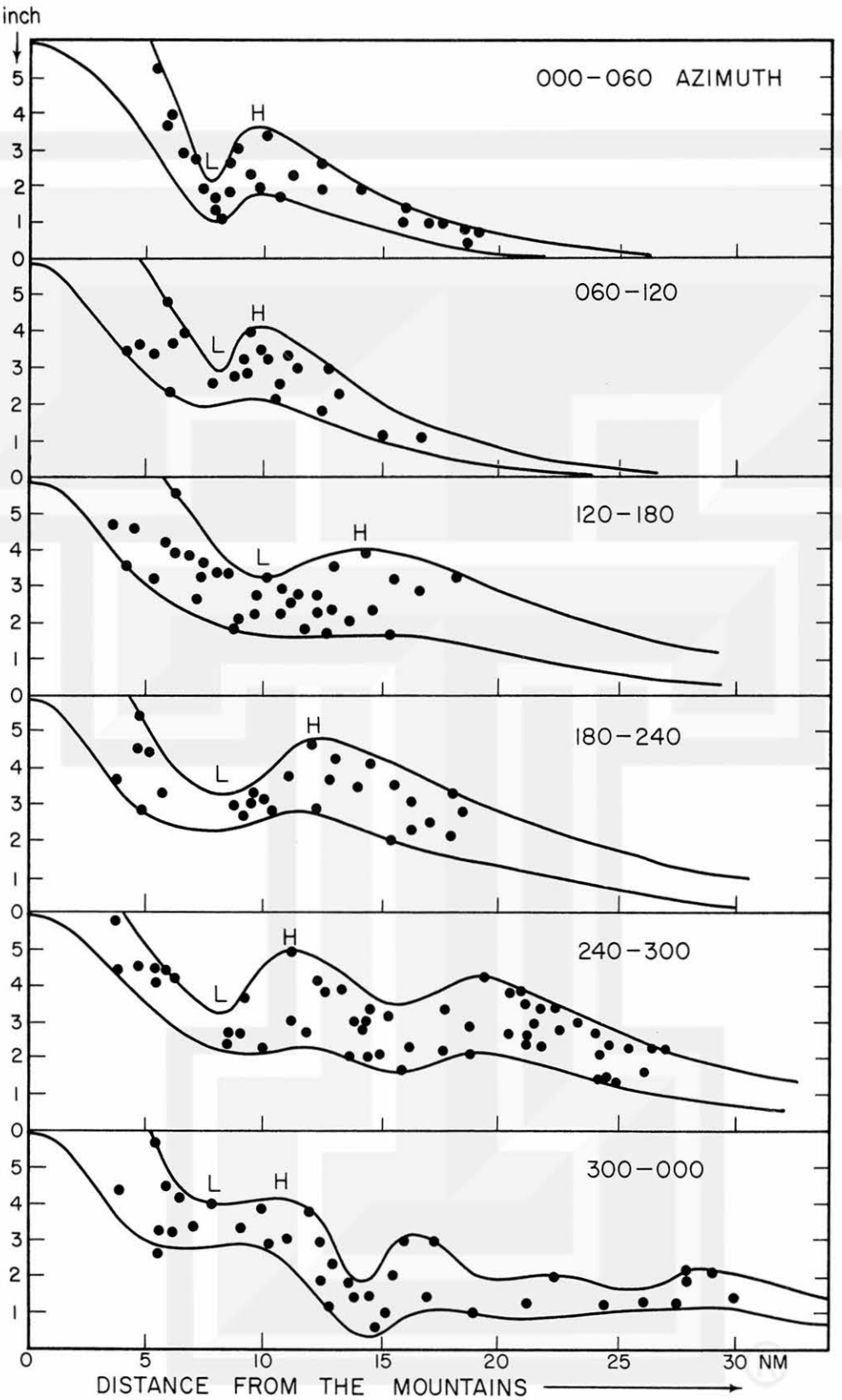

Fig. 6. Scatter diagrams showing the radial distribution of total rainfall around the San Francisco Mountains as measured during the 1961 season. The letter L indicates the position of the ring of low precipitation in each fan-shaped direction.

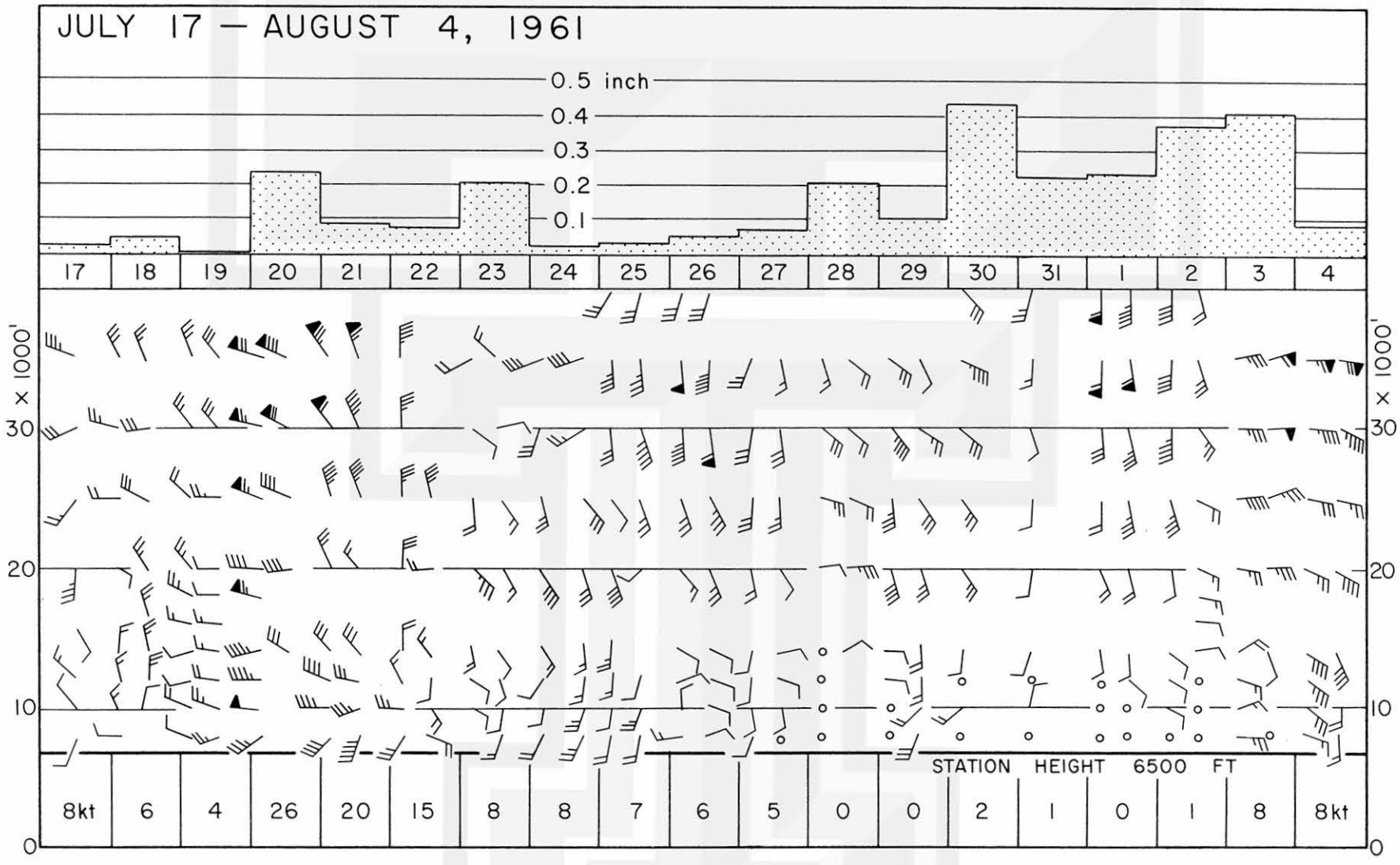

Fig. 7. Daily mean precipitation averaged over the network area compared with the winds aloft measured at the Flagstaff Airport by AFCRL. Winds were plotted in conventional symbols after doubling the wind speed; thus, one long barb = 5 kt and one flag = 25 kt. The daily wind speed entered below the station height line represents the mean wind below 10,000 ft measured early in the morning.

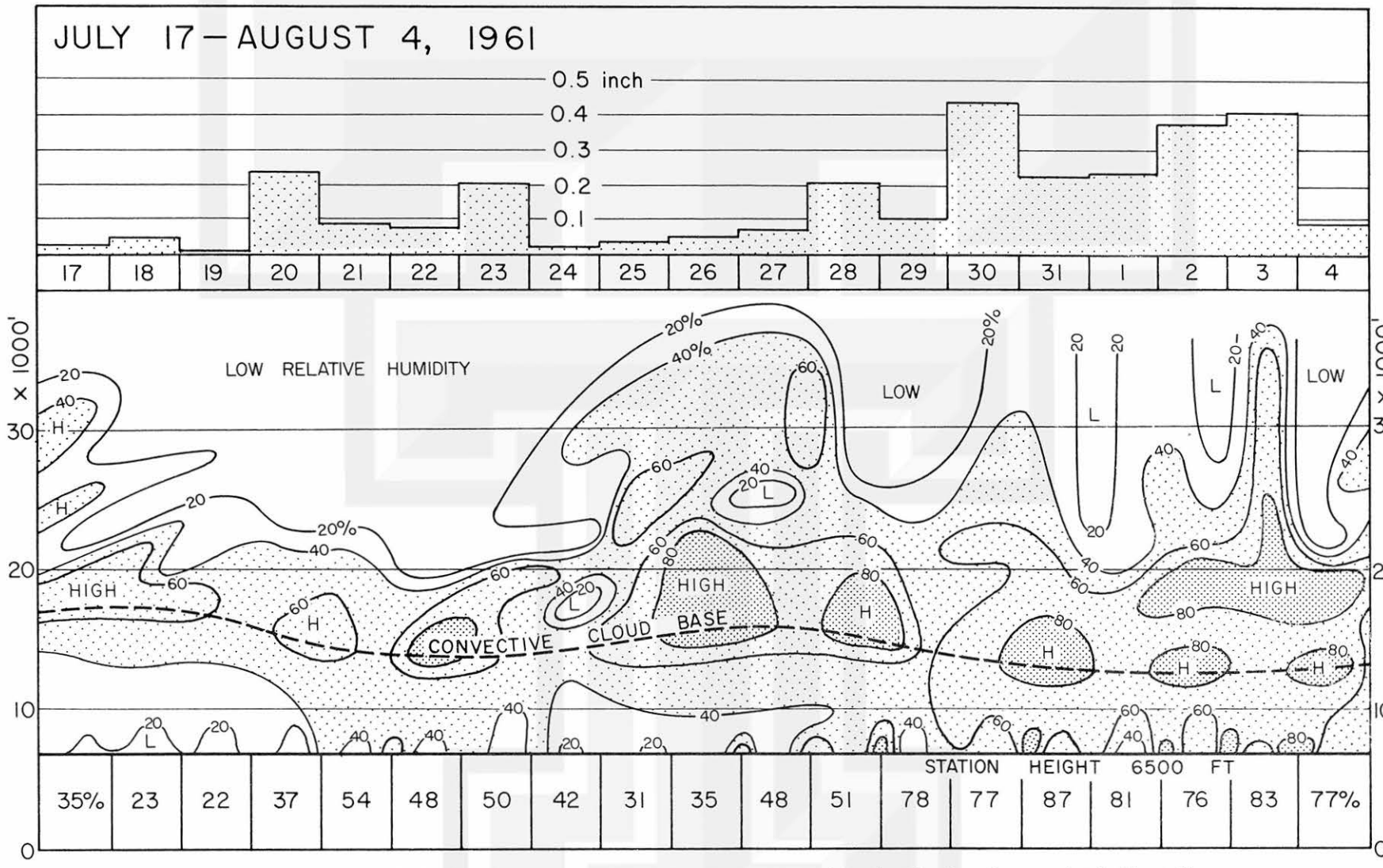

Fig. 8. Daily mean precipitation (upper) compared with the vertical distribution of relative humidity (lower) measured at the Flagstaff Airport by AFCRL. The relative humidity, measured by the GMD-1, was contoured for every 20%. Note that its diurnal variation extended to about 10,000 ft. Entered below the station elevation line (MSL) is the mean R.H. below 10,000 ft measured early in the morning.

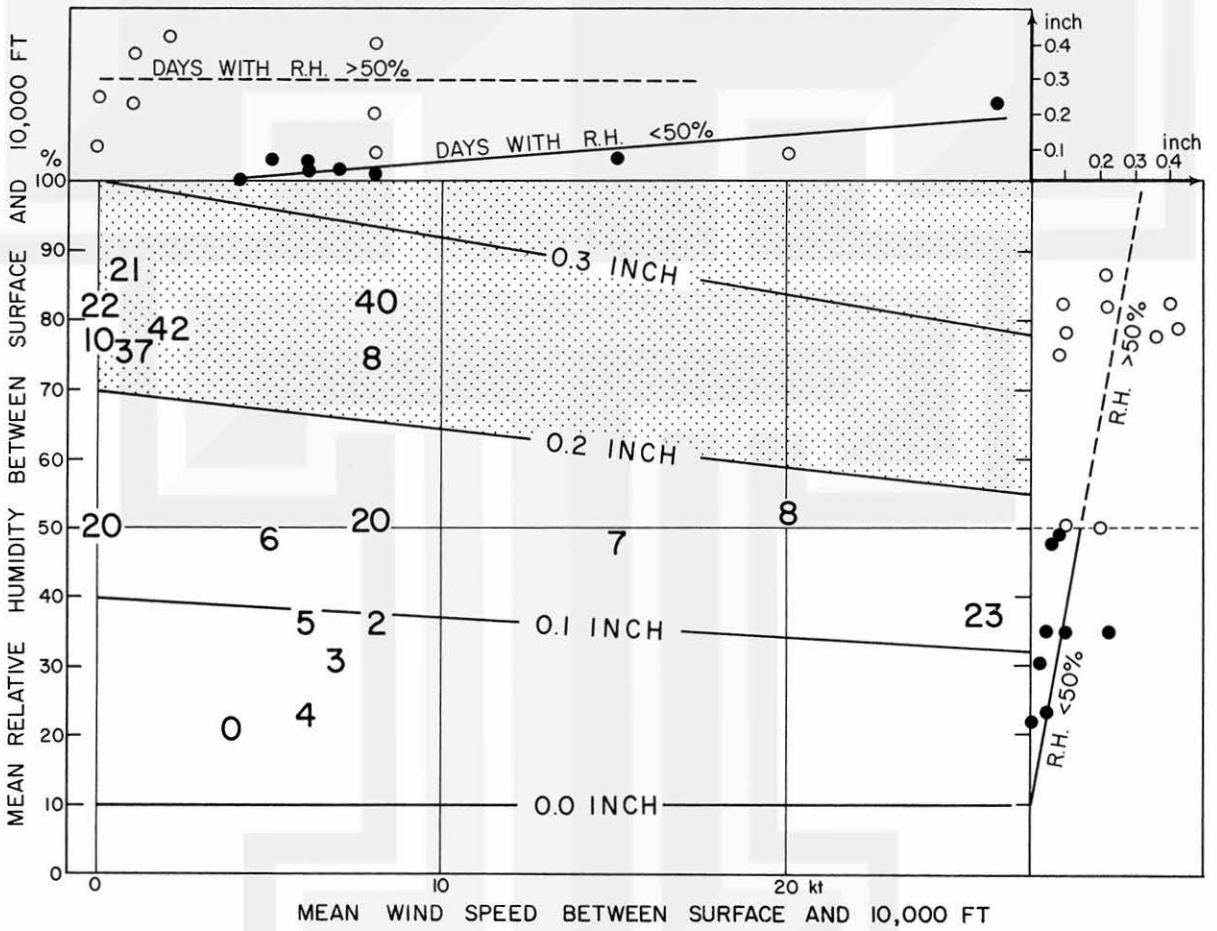

Fig. 9. Daily mean precipitation in 0.01-inch units plotted on relative humidity vs. wind speed coordinates. General trends of mean precipitation are contoured at 0.1-inch intervals from the empirical formula in the text. Solid and open circles in the R.H. vs. rainfall (right) and the wind speed vs. rainfall (upper) diagram represent the values with R.H. below and above 50%, respectively.

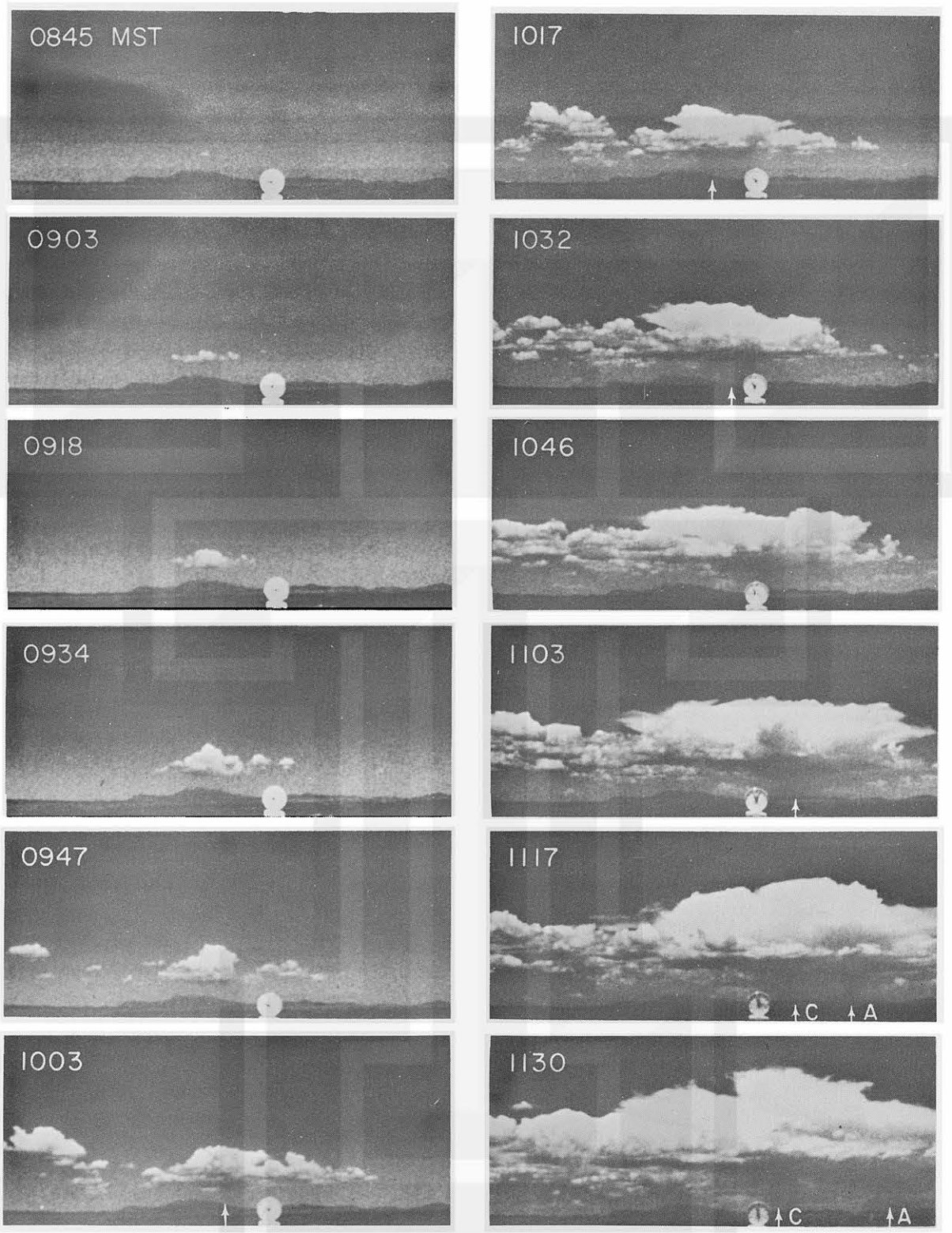

Fig. 10. Growth of orographic cumuli over the San Francisco Mountains on July 19, 1961. Note that a shower started at 1003 MST and gradually moved from left to right until 1103 MST when it split into A and C. Thereafter, C moved very slowly toward the left while A moved toward the right very fast. Such a motion of showers after the cloud split was computed by Fujita and Grandoso (1966) using their model of echo split.

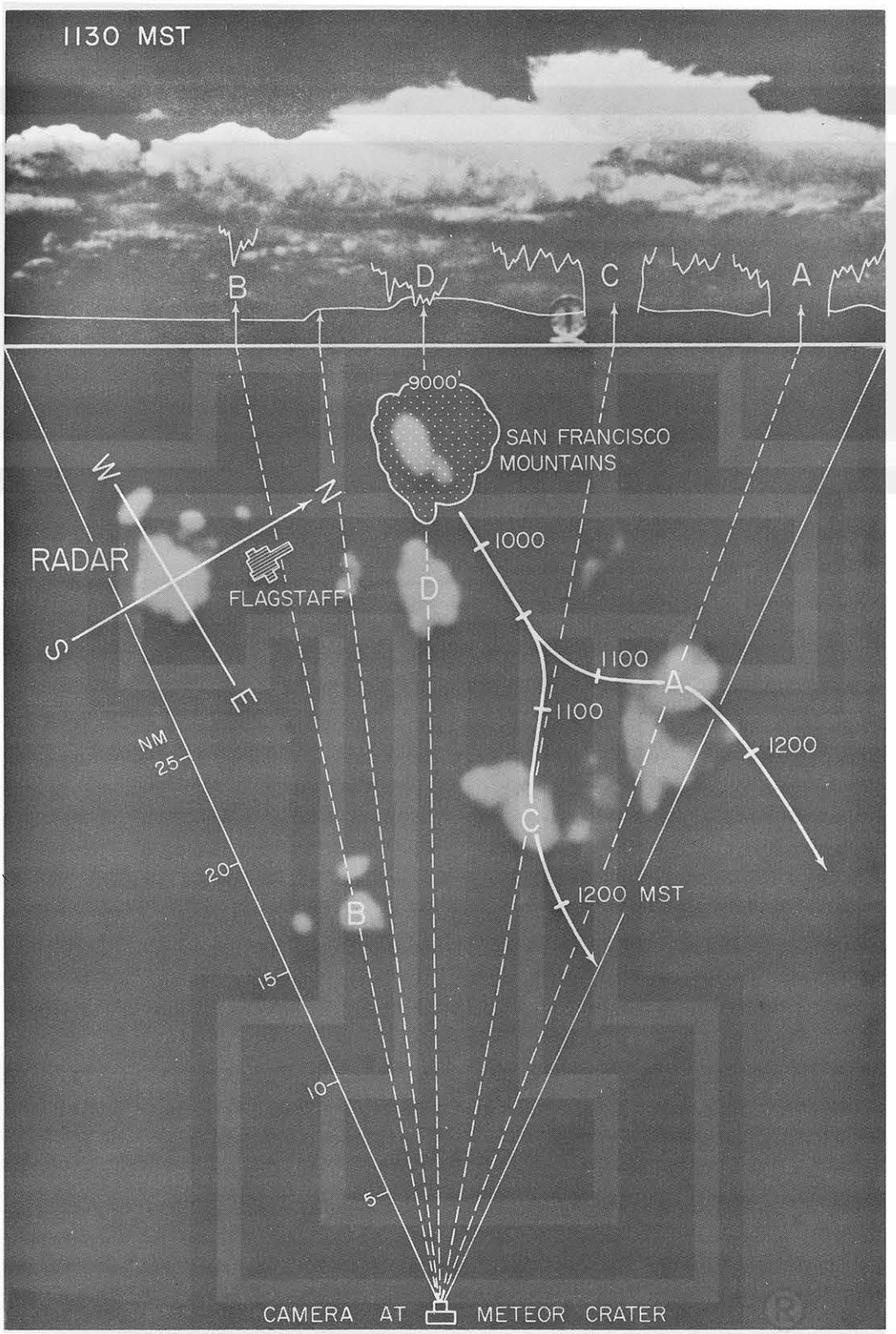

Fig. 11. A composite presentation of radar echoes and a cloud photograph taken from the rim of Meteor Crater, near Winslow, Arizona. The showers A and C in the cloud picture correspond to echoes A and C which were rotating in opposite directions. An anticyclonic rotation of echo A was very apparent for at least 30 min.

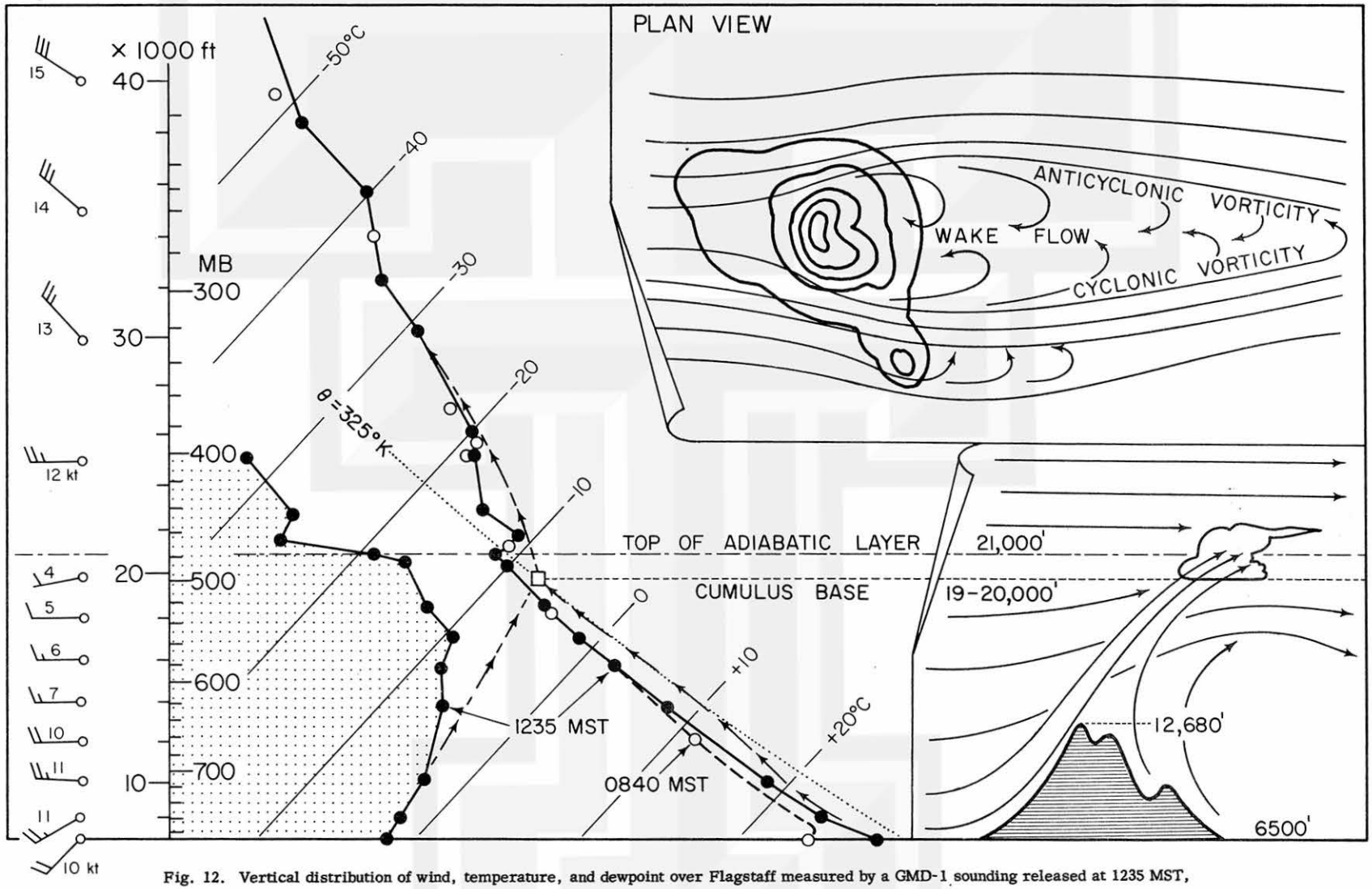

Fig. 12. Vertical distribution of wind, temperature, and dewpoint over Flagstaff measured by a GMD-1 sounding released at 1235 MST, July 19, 1961. 0840 MST temperatures are also entered for comparison. Short arrows in the adiabatic chart represent the schematic change in both T and Td of an air parcel rising diabatically along the slope of the San Francisco Mountains.

MESOMETEOROLOGY PROJECT - - - RESEARCH PAPERS

(Continued from front cover)

42. A Study of Factors Contributing to Dissipation of Energy in a Developing Cumulonimbus - Rodger A. Brown and Tetsuya Fujita
43. A Program for Computer Gridding of Satellite Photographs for Mesoscale Research - William D. Bonner
44. Comparison of Grassland Surface Temperatures Measured by TIROS VII and Airborne Radiometers under Clear Sky and Cirriform Cloud Conditions - Ronald M. Reap
45. Death Valley Temperature Analysis Utilizing Nimbus I Infrared Data and Ground-Based Measurements - Ronald M. Reap and Tetsuya Fujita
46. On the "Thunderstorm-High Controversy" - Rodger A. Brown
47. Application of Precise Fujita Method on Nimbus I Photo Gridding - Lt. Cmd. Ruben Nasta
48. A Proposed Method of Estimating Cloud-top Temperature, Cloud Cover, and Emissivity and Whiteness of Clouds from Short- and Long-wave Radiation Data Obtained by TIROS Scanning Radiometers - T. Fujita and H. Grandoso
49. Aerial Survey of the Palm Sunday Tornadoes of April 11, 1965 - Tetsuya Fujita
50. Early Stage of Tornado Development as Revealed by Satellite Photographs - Tetsuya Fujita
51. Features and Motions of Radar Echoes on Palm Sunday, 1965 - D. L. Bradbury and Tetsuya Fujita
52. Stability and Differential Advection Associated with Tornado Development - Tetsuya Fujita and Dorothy L. Bradbury
53. Estimated Wind Speeds of the Palm Sunday Tornadoes - Tetsuya Fujita
54. On the Determination of Exchange Coefficients: Part II - Rotating and Nonrotating Convective Currents - Rodger A. Brown
55. Satellite Meteorological Study of Evaporation and Cloud Formation over the Western Pacific under the Influence of the Winter Monsoon - K. Tsuchiya and T. Fujita
56. A Proposed Mechanism of Snowstorm Mesojet over Japan under the Influence of the Winter Monsoon - T. Fujita and K. Tsuchiya
57. Some Effects of Lake Michigan upon Squall Lines and Summertime Convection - Walter A. Lyons
58. Angular Dependence of Reflection from Stratiform Clouds as Measured by TIROS IV Scanning Radiometers - A. Rabbe
59. Use of Wet-beam Doppler Winds in the Determination of the Vertical Velocity of Raindrops inside Hurricane Rainbands - T. Fujita, P. Black and A. Loesch
60. A Model of Typhoons Accompanied by Inner and Outer Rainbands - Tetsuya Fujita, Tatsuo Izawa, Kazuo Watanabe, and Ichiro Imai

MESOMETEOROLOGY PROJECT - - - RESEARCH PAPERS

(Continued from inside back cover)

61. Three-Dimensional Growth Characteristics of an Orographic Thunderstorm System - Rodger A. Brown.

62. Split of a Thunderstorm into Anticyclonic and Cyclonic Storms and their Motion as Determined from Numerical Model Experiments - Tetsuya Fujita and Hector Grandoso.

63. Preliminary Investigation of Peripheral Subsidence Associated with Hurricane Outflow - Ronald M. Reap.

64. The Time Change of Cloud Features in Hurricane Anna, 1961, from the Easterly Wave Stage to Hurricane Dissipation - James E. Arnold.

65. Easterly Wave Activity over Africa and in the Atlantic with a Note on the Inter-tropical Convergence Zone during Early July 1961 - James E. Arnold.

66. Mesoscale Motions in Oceanic Stratus as Revealed by Satellite Data - Walter A. Lyons and Tetsuya Fujita.